BldC delays entry into development to produce a sustained period of vegetative growth in *Streptomyces venezuelae*

Matthew J. Bush[1,*], Mahmoud Al-Bassam[1,#], Govind Chandra[1], Kim C. Findlay[2] and Mark J. Buttner[1]

[1]*Department of Molecular Microbiology*, and [2]*Department of Cell and Developmental Biology, John Innes Centre, Norwich Research Park, Norwich NR4 7UH, UK.*

* To whom correspondence should be addressed. Tel: 44 (0) 1603 450757; Fax: 44 (0) 1603 450778; Email:matt.bush@jic.ac.uk

[#] Current address: Department of Paediatrics, University of California, San Diego, La Jolla, CA 92093, USA

Keywords: Morphological differentiation; sporulation; cell division; transcriptional regulation.

Abstract

Streptomycetes are filamentous bacteria that differentiate by producing spore-bearing reproductive structures called aerial hyphae. The transition from vegetative to reproductive growth is controlled by the *bld* (bald) loci, and mutations in *bld* genes prevent the formation of aerial hyphae, either by blocking entry into development (mutations in activators) or by inducing precocious sporulation in the vegetative mycelium (mutations in repressors). One of the *bld* genes, *bldC*, encodes a 68-residue protein with a winged Helix-Turn-Helix (wHTH) DNA-binding motif. Here we exploit the benefits of the new model species, *Streptomyces venezuelae*, which sporulates in liquid culture, to study the biological role of BldC. Using electron microscopy and time-lapse imaging, we show that *bldC* mutants are bald because they initiate development prematurely, bypassing the formation of aerial hyphae. This correlates with premature expression of BldC target genes, showing that BldC acts as a repressor to sustain vegetative growth and delay entry into development.

Introduction

The complex *Streptomyces* life cycle involves two distinct filamentous cell forms: the growing or vegetative hyphae and the reproductive or aerial hyphae, which differentiate into long chains of spores (1-5). Genetic studies identified the regulatory loci that control entry into development, which are called *bld* (bald) genes because null mutations in these loci prevent the formation of aerial hyphae. However, baldness can arise for two different reasons. The larger class of *bld* mutants, which define positive regulators, fail to initiate development, forming colonies of undifferentiated vegetative mycelium. In contrast, a smaller but growing class of *bld* mutants, which define negative regulators, enter development prematurely, inducing sporulation in the vegetative mycelium and bypassing the formation of aerial hyphae. Thus, macroscopically these two classes of mutants look similar, forming smooth colonies that lack the 'hairy' appearance of the wild type, but microscopically it is apparent that they arise for diametrically opposed reasons (4, 6-8).

bldC is known to encode a short, 68 residue protein related to the DNA-binding domain of MerR-family proteins (9), but there has been less insight into its biological role and impact on *Streptomyces* development. In part, this is because previous studies have focussed on the classical model species, *S. coelicolor*, which sporulates only on solid medium. Here we exploit the benefits of the new model species, *Streptomyces venezuelae*, which sporulates in liquid culture (10), to study the biological role of BldC. We show that *bldC* mutants are bald because they enter development prematurely, bypassing the formation of aerial hyphae. This correlates with premature expression of BldC target genes, showing that BldC acts as a repressor to sustain vegetative growth and delay entry into development.

Results

Deletion of *bldC* causes premature initiation of development

We constructed an *S. venezuelae bldC* mutant by replacing the *bldC* coding region with an apramycin resistance (*apr*) cassette. The resulting mutant was bald, unable to produce the reproductive aerial hyphae that give mature wild-type *Streptomyces* colonies their characteristic fuzzy appearance (Fig 1.). However, scanning electron microscopy (SEM) of mature colonies of the *bldC* mutant showed that most of the biomass consisted of spores, rather than undifferentiated vegetative hyphae (Fig. 2). Comparison of the growth of the wild type and the *bldC* mutant on plates over time showed that after 1 day they looked similar (vegetative growth only) but after 2 days the wild type had produced aerial hyphae while the *bldC* mutant was still restricted to vegetative growth. After 3 days, the aerial hyphae of the wild-type had differentiated into spores, and most of the biomass of the *bldC* mutant had also differentiated into spores, bypassing aerial mycelium formation. The *bldC* mutant also seemed to produce higher levels of extracellular matrix than the wild type (Fig. 2). The *bldC* mutant phenotype was fully complemented by introducing a single copy of the *bldC* gene under the control of its native promoter, expressed *in trans* from the ΦBT1 integration site (Figs. 1 and 2).

Using an established microfluidic system and methodology (10), we conducted fluorescence time-lapse microscopy to further study the developmental defects associated with deletion of *bldC*. As in previous studies (6,10), we introduced an FtsZ-YPet translational fusion into the wild type, mutant and complemented mutant strains, enabling us to monitor each of the two distinct modes of cell division that occur in *Streptomyces*. In Fig. 3, the scattered single Z-rings mark the position of vegetative cross-walls, which do not constrict or give rise to cell-cell separation, but simply divide the vegetative hyphae into long, box-like compartments (e.g. Figs. 3A + C, panel 2). In contrast, during reproductive growth, long ladders of regularly spaced

64 Z-rings are synchronously deposited along sporogenic hyphae. These Z-rings mark the sites of
65 sporulation septa, which do constrict, ultimately leading to the formation of chains of spores
66 (e.g. Figs. 3A + C, panels 3 +4). Time-lapse imaging of strains harbouring the FtsZ-YPet fusion
67 showed that the duration of vegetative growth was shorter in the *bldC* mutant compared to the
68 wild type and the complemented mutant (Fig.3 and Movies S1 A/B, S2 A/B and S3 A/B).
69 Noticeably, following germination, hyphal outgrowth in the *bldC* mutant was associated with
70 an immediate increase in FtsZ-YPet expression, leading to the precocious formation of ladders
71 of Z-rings (Fig. 3B and Movie S2A/B). However, although ladders of Z-rings were observed
72 as early as 4 hours in the *bldC* mutant, mature spores were not observed in the corresponding
73 DIC images until 21 hours, the same time mature spores were also seen in the wild type (Figs.
74 3A and B). Wild-type patterns of FtsZ expression and sporulation were restored in the
75 complemented mutant (Fig. 3C and Movie S3A/B). From these data, we concluded that the
76 overall role of BldC is to sustain vegetative growth and delay entry into development.
77

78 **BldC levels are highest early in development**

79 Using an anti-BldC polyclonal antibody, we monitored BldC levels in *S. venezuelae* during
80 sporulation in liquid culture. Western blotting showed that BldC is abundant throughout the
81 life cycle, but that BldC levels are highest early on, during vegetative growth (Figure 4).
82

83 **BldC represses transcription of its target genes *whiI* and *smeA***

84 ChIP-chip studies in *S. coelicolor* showed that BldC is a transcription factor and that it has a
85 large regulon of ~280 genes (11). These targets include many genes encoding key
86 transcriptional regulators of the *Streptomyces* developmental cascade (e.g. *bldM*, *whiB*, *whiD*,
87 *whiH*, *whiI*, *sigF* and *bldC* itself), as well as others encoding proteins involved in chromosome
88 condensation and segregation during sporulation (e.g. *hupS*, *smeA-sffA*). Schumacher et al. (11)

89 characterised the interaction of *S. coelicolor* BldC with the promoters of two of its targets, *whiI*
90 and the *smeA-ssfA* operon. *whiI* encodes an orphan response-regulator that is essential for the
91 later stages of sporulation, when it forms a functional heterodimer with a second orphan
92 response-regulator, BldM, enabling WhiI to bind to DNA and regulate the expression of ~40
93 late sporulation genes (12). The *smeA-sffA* operon encodes a small membrane protein (SmeA)
94 that recruits a DNA translocase (SffA) to sporulation septa (13). Deletion of *smeA-sffA* results
95 in a defect in spore chromosome segregation and has pleiotropic effects on spore maturation
96 (13).

97 BldC directly regulates the *whiI* and *smeA* promoters in *S. coelicolor* (11) and ChIP-chip
98 analysis confirmed that they are also BldC targets in *S. venezuelae* (Table S1, Fig. 5). To assess
99 the regulatory influence of BldC on the *whiI* and *smeA* promoters, we performed qRT-PCR
100 using RNA prepared from both wild-type *S. venezuelae* and the *bldC* mutant at time points
101 throughout differentiation in liquid culture (Fig. 6). In the wild type, expression of both BldC
102 targets comes on in the 14-h time point. In contrast, in the *bldC* mutant, expression of both *whiI*
103 and *smeA* is on in the 8- and 10-h time points. We conclude that BldC functions to repress the
104 transcription of these target genes during early vegetative growth.

105

106 **Discussion**

107 Canonical *bld* mutations block entry into development and so the resulting colonies do not
108 form aerial hyphae and spores. Such mutations typically define positive regulators such as the
109 response regulator BldM (12) or the sigma factor BldN (14). In contrast, we have shown that
110 *S. venezuelae bldC* mutants are bald because they enter development prematurely, bypassing
111 the formation of aerial hyphae, and that this correlates with premature expression of BldC target
112 genes like *whiI* and *smeA*. Thus, BldC functions as a repressor to sustain vegetative growth and

113 delay entry into development. As such, BldC joins a growing class of Bld regulators known to
114 function as a developmental "brake".

115 BldD was the first Bld regulator of this alternative class to be clearly recognized. BldD sits at
116 the top of the developmental cascade and represses a large regulon of ~170 sporulation genes
117 during vegetative growth. BldD activity is controlled by the second messenger c-di-GMP,
118 which mediates dimerization of two BldD protomers to generate a functional repressor. In this
119 way, c-di-GMP signals through BldD to repress expression of the BldD regulon, extending
120 vegetative growth and inhibiting entry into development (4, 8, 15). Because it is a BldD-(c-di-
121 GMP) complex that represses the BldD regulon and not BldD alone, engineering the
122 degradation of c-di-GMP *in vivo* also causes a precocious hypersporulation phenotype like that
123 of a *bldD* null mutant (8).

124 More recently, *bldO* was identified as a second member of this emerging class of *bld* mutant
125 (6-7). In contrast to BldD and BldC, which both control large regulons, BldO functions to
126 repress a single developmental gene, *whiB*. The precocious hypersporulation phenotype of the
127 *bldO* mutant arises from premature expression of *whiB*, and in line with this, constitutive
128 expression of *whiB* alone is sufficient to induce precocious hypersporulation in wild-type *S.*
129 *venezuelae* (6). WhiA and WhiB act together to co-control the same set of promoters to initiate
130 developmental cell division in *Streptomyces* (16-17). WhiA is constitutively present
131 throughout the life cycle, but it only binds to its target promoters at the onset of sporulation
132 (16). This is because WhiA and WhiB function cooperatively and *in vivo* DNA binding by
133 WhiA depends on WhiB, and *vice versa* (17). As a consequence, the regulation of *whiB*
134 expression is key in controlling the switch between hyphal growth and sporulation. This critical
135 role for WhiB is reflected in the extensive developmental regulation to which *whiB*
136 transcription is subject, being directly repressed by BldC (11), BldD (18) and BldO (6), and
137 directly activated by BldM (12).

138 **Materials and Methods**

139 **Construction and complementation of an *S. venezuelae bldC* null mutant.** Using 'Redirect'
140 PCR targeting (19-20), *bldC* mutants were generated in which the coding region was replaced
141 with a single apramycin resistance (*apr*) cassette. A cosmid library that covers > 98% of the *S.*
142 *venezuelae* genome (M.J. Bibb and M.J. Buttner, unpublished) is fully documented at
143 http://strepdb.streptomyces.org.uk/. Cosmid 4O24 was introduced into *E. coli* BW25113
144 containing pIJ790 and the *bldC* gene (*sven3846*) was replaced with the *apr-oriT* cassette
145 amplified from pIJ773 using the primer pairs bldCdis_F and bldCdis_R. The resulting
146 disrupted cosmids were confirmed by restriction digestion and by PCR analysis using the
147 flanking primers bldCcon_F and bldCcon_R, and introduced into *S. venezuelae* by conjugation
148 (Keiser *et al*., 2000). Null mutant derivatives, generated by double crossing over, were
149 identified by their apramycin-resistant, kanamycin-sensitive and morphological phenotypes,
150 and their chromosomal structures were confirmed by PCR analysis using the flanking primers
151 bldCcon_F and bldCcon_R. A representative *bldC* null mutant was designated SV25. For
152 complementation, *bldC* was amplified with the primers bldCcomp_F and bldCcomp_R,
153 generating an 846bp fragment carrying the coding sequence and the *bldC* promoter, and cloned
154 into HindIII-KpnI/Asp718 cut pIJ10770 to create pIJ10618. The plasmid was introduced into
155 the *bldC* mutant by conjugation and fully complemented all aspects of the mutant phenotype.

156

157 **Time-lapse imaging of *S. venezuelae*.** Fluorescent time-lapse imaging was conducted
158 essentially as described previously (6,11). Before imaging, fresh *S. venezuelae* spores for each
159 of the strains imaged were first prepared by inoculating 30 ml cultures of MYM with 10 µl of
160 the appropriate spore stock or 20 µl of the appropriate mycelial culture. Cells were cultured at
161 30 ºC and 250 rpm until fully differentiated (16-24 h for hypersporulating strains, otherwise
162 36-40 h). 1 ml of each culture was spun briefly to pellet mycelium, the supernatant spores were

163 diluted 1:50 in fresh MYM, and 50 µl was transferred to the cell loading well of a prepared
164 B04A microfluidic plate (Merck-Millipore). The remaining culture was filter-sterilised to
165 obtain spent MYM that was free of spores and mycelial fragments. The ONIX manifold was
166 then sealed to the B04A plate before transferring to the environmental chamber, pre-incubated
167 at 30 ºC. Spores were loaded onto the B04A plate, at 4 psi for 15 seconds using the ONIX
168 microfluidic perfusion system. Fresh MYM medium was set to flow at 2 psi during the first 3
169 hours during germination, before the 2-psi flow of spent MYM medium for the remainder of
170 the experiment. The system was left to equilibrate for 1 h prior to imaging.
171
172 Imaging was conducted using a Zeiss Axio Observer.Z1 widefield microscope equipped with
173 a sCMOS camera (Hamamatsu Orca FLASH 4), a metal-halide lamp (HXP 120V), a hardware
174 autofocus (Definitive Focus), a 96-well stage insert, an environmental chamber, a 100x 1.46
175 NA Oil DIC objective and the Zeiss 46 HE shift free (excitation500/25 nm, emission 535/30
176 nm) filter set. DIC images were captured with a 150 ms exposure time, YFP images were
177 captured with a 100 ms exposure time. Images were taken every 30 min. In all experiments,
178 multiple x/y positions were imaged for each strain and in each experiment. Representative
179 images were transferred to the Fiji software package (http://fiji.sc/Fiji), manipulated and
180 converted into the movie files presented here, as described previously (Schlimpert *et al*., 2016).
181
182 **Chromatin immunoprecipitation-microarray (ChIP-chip) analysis.** To carry out the ChIP-
183 chip experiments, cultures of *S. venezuelae* and the congenic *bldC* null mutant strain SV25
184 were grown for 12 h in MYM liquid medium. Formaldehyde was added to cultures at a final
185 concentration of 1% (v/v) and incubation was continued for 30 min. Glycine was then added
186 to a final concentration of 125 mM to stop the cross-linking. Cultures were left at room
187 temperature (RT) for 5 min before the mycelium was harvested and washed twice in PBS buffer

188 pH 7.4. Each mycelial pellet was resuspended in 0.5 ml lysis buffer (10 mM Tris HCl pH 8.0,
189 50 mM NaCl) containing 15 mg/ml lysozyme and protease inhibitor (Roche Applied Science)
190 and incubated at 25 ºC for 1 h. An equal volume of IP buffer (100 mM Tris HCl pH 8, 250 mM
191 NaCl, 0.5% Triton-X-100, 0.1% SDS) containing protease inhibitor was added and samples
192 were chilled on ice. Samples were sonicated for 7 cycles of 15 s each at 10 microns to shear
193 the chromosomal DNA into fragments ranging from 300-1000 bp in size. Samples were
194 centrifuged twice at 13,000 rpm at 4 ºC for 15 min to clear the cell extract, after which 10 µl
195 of cell extract was set aside for total DNA extraction. The remainder was incubated with 10%
196 (v/v) protein A-sepharose (Sigma) for 1 h on a rotating wheel to remove non-specifically
197 binding proteins. Samples were then centrifuged for 15 min at 4ºC and 13,000 rpm to remove
198 the beads. Supernatants were incubated with 10% (v/v) anti-BldC antibody (9) overnight at 4
199 ºC with rotation. Subsequently, 10% (v/v) protein A-sepharose was added to precipitate BldC
200 and incubation was continued for 4 h. Samples were centrifuged at 3500 rpm for 5 min and the
201 pellets were washed four times with 0.5x IP buffer. Each pellet was incubated overnight at 65
202 ºC in 150 µl IP elution buffer (50 mM Tris HCl pH 7.6, 10 mM EDTA, 1% SDS) to reverse
203 cross-links, and 10 µl of the total cell extract control was treated in the same way. Samples
204 were centrifuged at 13,000 rpm for 5 min to remove the beads. Each pellet was re-extracted
205 with 50 µl TE buffer (10 mM Tris HCl pH 7.4, 1 mM EDTA) and the supernatant incubated
206 with 0.2 mg/ml Proteinase K (Roche) for 2 h at 55ºC. The resulting samples were extracted
207 with phenol-chloroform and further purified using QiaQuick columns, eluting in 50 µl EB
208 buffer (Qiagen). DNA labelling, hybridization to DNA microarrays and data processing were
209 carried out as described previously (10).
210
211 **qRT-PCR.** Mycelial pellets from MYM cultures were washed in PBS and resuspended in 900
212 µl lysis solution (400 µl phenol [pH4.3], 100 µl chlorophorm:isoamyl alcohol (24 : 1) and 400

213 µl RLT buffer [Qiagen]) with lysing matrix B (MP Biomedicals) and homogenised using a
214 FastPrep FP120 Cell Disruptor (Thermo Savant). Two pulses of 30 s of intensity 6.0 were
215 applied with cooling down for 1 min on ice between pulses. Supernatants were centrifuged for
216 15 min, full-speed on a bench-top centrifuge at 4°C and then treated according to the
217 instructions given in the RNEasy Kit (Qiagen). The RNA samples were treated with on-column
218 DNase I (Qiagen), followed by an additional DNase I treatment (Turbo DNA-free, Ambion)
219 until they were free of DNA contamination (determined by PCR amplification of *hrdB*). RNA
220 was quantified and equal amounts (350 ng) of total RNA from each sample was converted to
221 cDNA using SuperScript II reverse transcriptase and random primers (Invitrogen). cDNA was
222 then used as template in qRT-PCR performed using the SensiFAST SYBR No-ROX kit
223 (Bioline). Three technical replicates were used for each gene. Specific qPCR primers (Table
224 S1, final concentration of 250 nM) were used to amplify the *whiI* target gene (whiIqRT_F and
225 whiIqRT_R), the *smeA* target gene (smeAqRT_F and smeAqRT-R) the *hrdB* reference gene
226 (hrdBqRT_F and hrdBqRT_R). To normalize for differing primer efficiency, a standard curve
227 was constructed using chromosomal DNA. Melting curve analysis was used to confirm the
228 production of a specific single product from each primer pair. qRT-PCR was performed using
229 a CFX96 Touch instrument using hardshell white PCR plates (BioRad), sealed with
230 thermostable film covers (Thermo). PCR products were detected with SYBR green fluorescent
231 dye and amplified according to the following protocol: 95°C, 3 min, then 45 cycles at 95°C 5
232 sec, 60°C 10 sec and 72°C 7 sec. Melting curves were generated at 65 to 95°C with 0.5°C
233 increments. The BioRad CFX manager software was used to calculate starting quantity (SQ)
234 values for *smeA* and *whiI* at each time point. These values were divided by the mean SQ value
235 derived from the *hrdB* reference at the corresponding time points, generating a value for
236 relative expression. The resulting values were normalised against the mean relative expression
237 of the wild type at 8 hours, which was set to 1.

238 **Western Blotting.** Samples of frozen mycelium, originating from 2 ml liquid MYM samples,
239 were resuspended in 0.4 ml ice-cold sonication buffer [20 mM Tris pH 8.0, 5 mM EDTA, 1 x
240 EDTA-free protease inhibitors (Roche)] and sonicated (5x 15 sec on/15 sec off) at 4.5 micron
241 amplitude. Lysates were then centrifuged at 16,000 xg for 15 min at 4˚C to remove cell debris.
242 Total protein concentration was determined using the Bradford assay (Biorad). 1 µg of total
243 protein from each time point was loaded in triplicate into a microplate (proteinsimple #043-
244 165) and anti-bldC antibody (9) diluted 1:200. BldC levels, originating from the wild type
245 strain and the *bldC* mutant negative control were then assayed using the automated Western
246 blotting machine Wes (ProteinSimple, San Jose, CA), according to the manufacturer's
247 guidelines.
248 **Scanning electron microscopy.** Colonies were mounted on the surface of an aluminum stub
249 with optimal cutting temperature compound (Agar Scientific Ltd, Essex, UK), plunged into
250 liquid nitrogen slush at approximately -210°C to cryopreserve the material, and transferred to
251 the cryostage of an Alto 2500 cryotransfer system (Gatan, Oxford, England) attached to a FEI
252 NanoSEM 450 field emission gun scanning electron microscope (FEI Ltd, Eindhoven, The
253 Netherlands). The surface frost was sublimated at -95°C for 3½ mins before the sample was
254 sputter coated with platinum for 2 min at 10 mA at below -110°C. Finally, the sample was
255 moved onto the cryostage in the main chamber of the microscope, held at approximately -
256 130°C, and viewed at 3 kV.
257
258
259

Acknowledgements

We are grateful to Oxford Gene Technology for expert handling of the ChIP samples. This work was funded by BBSRC grant BB/H006125/1 (to M.J.B.) and by BBSRC Institute Strategic Programme Grant BB/J004561/1 to the John Innes Centre.

265 **References**

266 1. Flärdh K, Buttner MJ. 2009. *Streptomyces* morphogenetics: dissecting differentiation in a
267 filamentous bacterium. Nat Rev Microbiol 7: 36-49.

268 2. McCormick JR, Flärdh K. 2012. Signals and regulators that govern *Streptomyces*
269 development. FEMS Microbiol Rev 36: 206-231.

270 3. Jakimowicz D, and van Wezel GP. 2012. Cell division and DNA segregation in
271 *Streptomyces*: how to build a septum in the middle of nowhere? Mol Microbiol 85: 393-404.

272 4. Bush MJ, Tschowri N, Schlimpert S, Flärdh K, Buttner MJ. 2015. c-di-GMP signaling and
273 the regulation of developmental transitions in *Streptomyces*. Nat Rev Microbiol 13: 749-760.

274 5. Chater KF. 2016. Recent advances in understanding *Streptomyces*. F1000Res 5: 2795.

275 6. Bush MJ, Chandra G, Findlay KC, Buttner MJ. 2017. Multi-layered inhibition of
276 *Streptomyces* development: BldO is a dedicated repressor of whiB. Mol. Microbiol. 104: 700-
277 711.

278 7. Flärdh K, McCormick JR. 2017. The *Streptomyces* O-B one connection: a force within
279 layered repression of a key developmental decision. Mol. Microbiol 104: 695-699.

280 8. Tschowri N, Schumacher MA, Schlimpert S, Chinnam NB, Findlay KC, Brennan RG,
281 Buttner MJ. 2014. Tetrameric c-di-GMP mediates effective transcription factor dimerization
282 to control *Streptomyces* development. Cell 158: 1136-1147.

283 9. Hunt AC, Servin-Gonzalez L, Kelemen GH, Buttner MJ. 2005. The bldC developmental
284 locus of *Streptomyces coelicolor* encodes a member of a family of small DNA-binding proteins
285 related to the DNA-binding domains of the MerR family. J Bacteriol 187: 716-728.

286 10. Schlimpert S, Flärdh K, Buttner, MJ. 2016. Fluorescence time-lapse imaging of the
287 complete *Streptomyces* life cycle using a microfluidic device. J Vis Exp 108: e53863.

288 11. Schumacher MA, den Hengst CD, Bush MJ, Le TB, Tran NT, Chandra G, Zeng W, Travis
289 B, Brennan RG, Buttner MJ. 2017. Manuscript in preparation.

290 12. Al-Bassam MM, Bibb MJ, Bush MJ, Chandra G, Buttner MJ. 2014. Response regulator
291 heterodimer formation controls a key stage in *Streptomyces* development. PLoS Genet 10:
292 e1004554.

293 13. Ausmees N, Wahlstedt H, Bagchi S, Elliot MA, Buttner MJ, Flärdh K. 2007. SmeA, a small
294 membrane protein with multiple functions in *Streptomyces* sporulation including targeting of a
295 SpoIIIE/FtsK-like protein to cell division septa. Mol Microbiol 65:1458-1473.

296 14. Bibb MJ, Domonkos A, Chandra G, Buttner MJ. 2012. Expression of the chaplin and rodlin
297 hydrophobic sheath proteins in *Streptomyces venezuelae* is controlled by σ^{BldN} and a cognate
298 anti-sigma factor, RsbN. Mol. Microbiol. 84:1033–1049.

299 15. Schumacher MA, Zeng W, Findlay KC, Buttner MJ, Brennan RG, Tschowri N. 2017. The
300 *Streptomyces* master regulator BldD binds c-di-GMP sequentially to create a functional $BldD_2$-
301 $(c\text{-di-GMP})_4$ complex. Nucleic Acids Res 45: 6923-6933.

302 16. Bush MJ, Bibb MJ, Chandra G, Findlay KC, Buttner MJ. 2013. Genes required for aerial
303 growth, cell division, and chromosome segregation are targets of WhiA before sporulation in
304 *Streptomyces venezuelae*. mBio 4: e00684-13.

305 17. Bush MJ, Chandra G, Bibb MJ, Findlay KC, Buttner MJ. 2016. Genome-wide chromatin
306 immunoprecipitation sequencing analysis shows that WhiB is a transcription factor that co-
307 controls its regulon with WhiA to initiate developmental cell division in *Streptomyces*. mBio
308 7: e00523-16.

309 18. den Hengst CD, Tran NT, Bibb MJ, Chandra C, Leskiw BK, Buttner MJ. 2010. Genes
310 essential for morphological development and antibiotic production in *Streptomyces coelicolor*
311 are targets of BldD during vegetative growth. Mol Microbiol 78: 361-379.

312 19. Gust B, Challis GL, Fowler K, Kieser T, Chater KF. 2003 PCR-targeted *Streptomyces* gene
313 replacement identifies a protein domain needed for biosynthesis of the sesquiterpene soil odor
314 geosmin. Proc Natl Acad Sci USA 100**:** 1541-1546.
315 20. Gust B, Chandra G, Jakimowicz D, Yuqing T, Bruton C, Chater KF. 2004. Lambda red-
316 mediated genetic manipulation of antibiotic-producing *Streptomyces*. Adv Appl Microbiol 54:
317 107-128.

318 **Figure Legends**

319 **FIG 1.** BldC is required for the formation of aerial mycelium.

320 The phenotypes of wild-type *S.venezuelae*, the *bldC* mutant, the *bldC* mutant carrying the
321 empty vector, and the complemented *bldC* mutant, photographed after four days of growth on
322 MYM solid medium.

323

324 **FIG 2.** Deletion of *bldC* causes premature initiation of development on solid medium.

325 Scanning electron micrographs showing the phenotype of the *bldC* mutant, compared to wild-
326 type after 1 days, 2 days and 3 days of growth on MYM solid medium. The phenotype of the
327 complemented *bldC* mutant is also shown after 3 days of growth on MYM solid medium.

328

329 **FIG 3.** Deletion of *bldC* causes premature initiation of development in liquid medium.

330 Time-lapse images (4, 7, 12 and 21 h post-inoculation) of (A) wild-type *S. venezuelae*, (B) the
331 *bldC* mutant and (C) the complemented *bldC* mutant, grown in liquid MYM medium in the
332 microfluidic system. All three strains carry the same FtsZ-YPet translational fusion expressed
333 from the native ftsZ promoter, and both the DIC (upper) and fluorescence (lower) images are
334 shown. Scale Bar = 10µm. For the corresponding movies, please see Supporting Information
335 Movies S1A/B, S2A/B and S3 A/B.

336

337 **FIG 4.** Automated Western blot analysis of BldC.

338 Equal amounts (1 µg) of total protein were loaded for each sample and BldC was detected with
339 polyclonal antibody (9) using the quantitative 'Wes' capillary electrophoresis and blotting
340 system (ProteinSimple – San Jose, CA). The *S. venezuelae bldC* mutant was used as a negative
341 control. Both the wild-type and *bldC* mutant were grown in MYM liquid medium. (A)
342 quantitation of BldO levels (area under each peak; arbitrary units). (B) virtual Western blot.

343 All experimental samples were analysed in triplicate and the mean value and its Standard Error
344 are shown for each sample. Each time-point is indicated in hours, along with its relation to the
345 developmental stage (V = vegetative growth; F = fragmentation; S = sporulation), as
346 determined by microscopy. Cultures used to analyse BldC levels were identical to those used
347 to prepare RNA prior to qRT-PCR analysis (Fig. 6).
348
349 **FIG 5.** BldC regulates the expression of many genes in *S. venezuelae*.
350 (A) Genome-wide distribution of BldC binding sites identified by ChIP-chip analysis using
351 anti-BldC polyclonal antibody, conducted during vegetative growth (12 hr) in the wild type.
352 DNA obtained from immunoprecipitation of BldC was labelled with Cy3 and hybridized to
353 DNA microarrays together with a total DNA control labelled with Cy5. Data are plotted as
354 Cy3/Cy5 ratios (y-axis), as a function of chromosome location (x-axis).
355 (B) ChIP-chip data for *whiI* and *smeA* in wild-type *S. venezuelae* and the *S. venezuelae ΔbldC*
356 mutant (blue and red dots, respectively). Plots span approximately 8 kb of DNA sequence.
357 Genes running left to right are shown in green, and genes running right to left are shown in red.
358 The black arrow indicates the gene subject to BldC regulation.
359
360 **FIG 6.** BldC functions to repress transcription. *whiI* (A) and *smeA* (B) mRNA abundance
361 determined by qRT-PCR in the wild type (white bars) and the bldC mutant (black bars)
362 throughout development. Strains were grown in MYM liquid medium. Expression values were
363 calculated relative to the accumulation of the constitutively expressed *hrdB* reference mRNA
364 and normalised to the wild-type value at 8 h. Cultures used to prepare RNA prior to qRT-PCR
365 analysis were identical to those used to analyse BldC levels (Fig. 4).
366

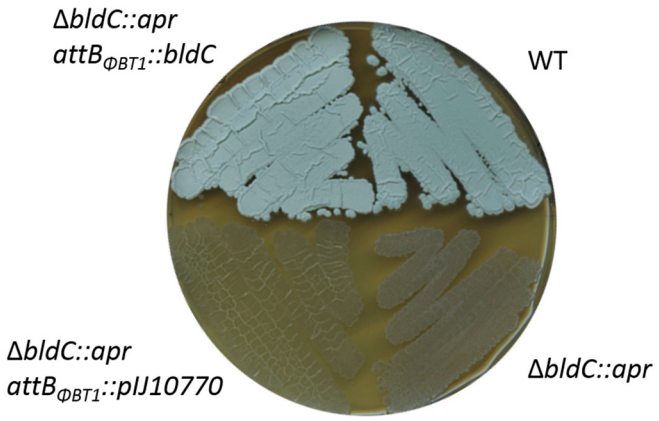
ΔbldC::apr
attB$_{\Phi BT1}$::bldC
WT
ΔbldC::apr
attB$_{\Phi BT1}$::pIJ10770
ΔbldC::apr

FIG 1

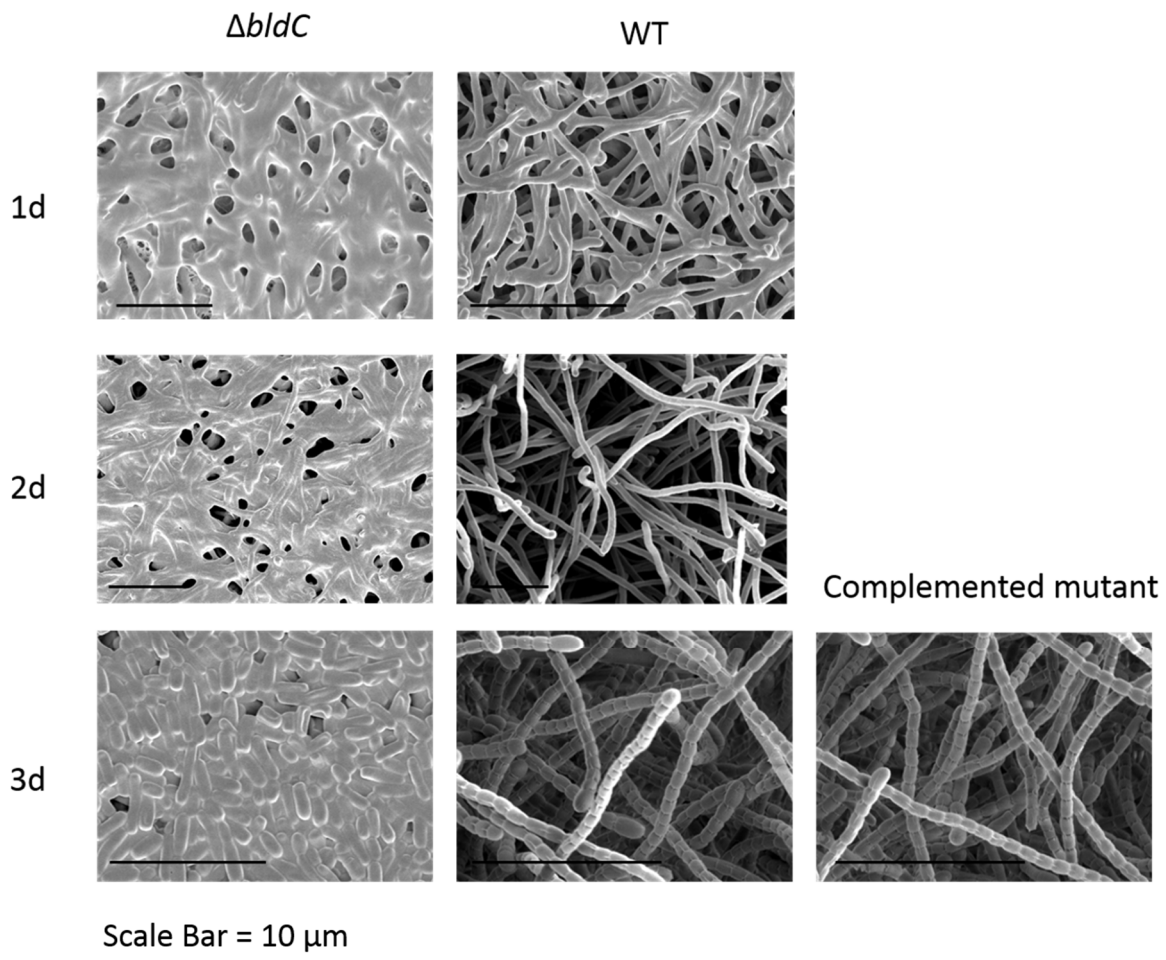

FIG 2.

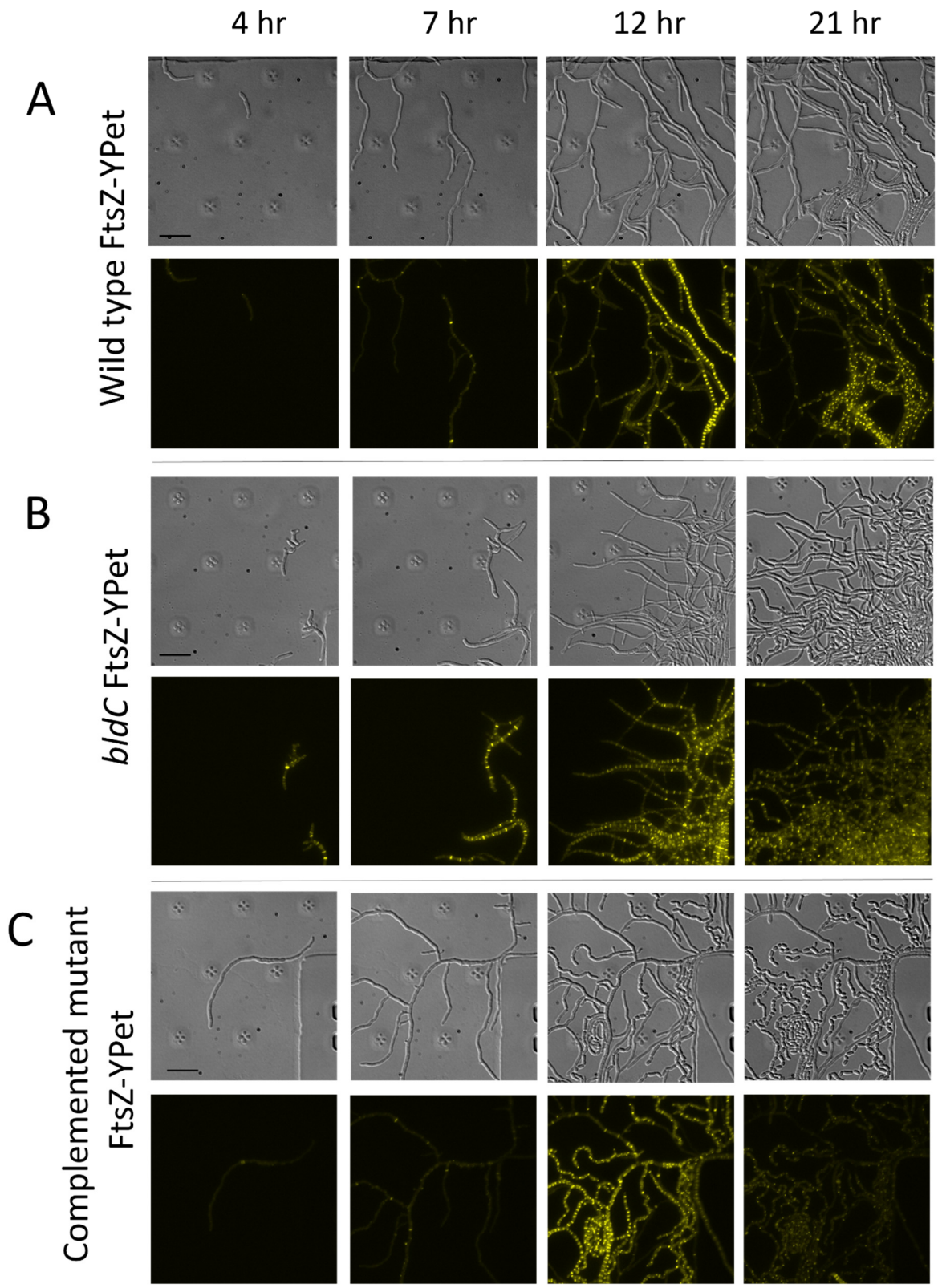
4 hr
7 hr
12 hr
21 hr
A
Wild type FtsZ-YPet
B
bldC FtsZ-YPet
C
Complemented mutant FtsZ-YPet

FIG 3.

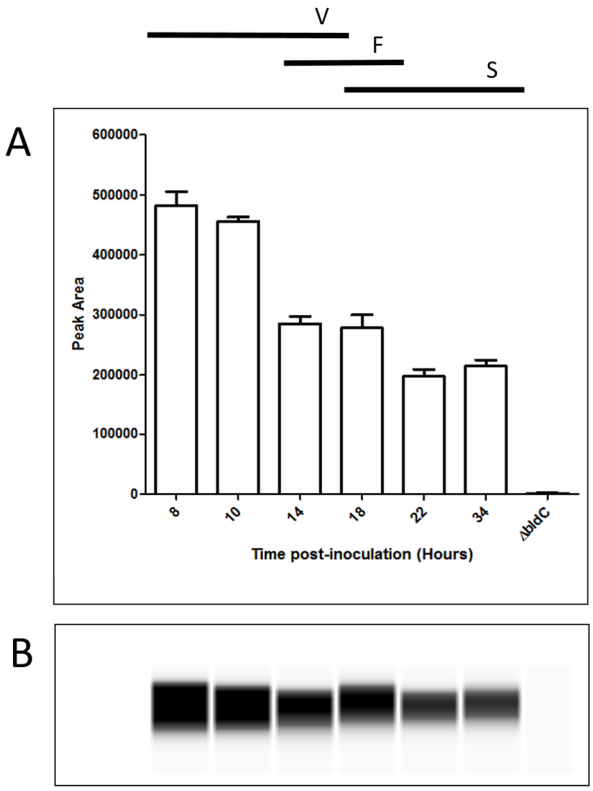
V
F
S
A
600000
500000
400000
300000
200000
100000
0
Peak Area
8
10
14
18
22
34
ΔbldC
Time post-inoculation (Hours)
B

FIG 4.

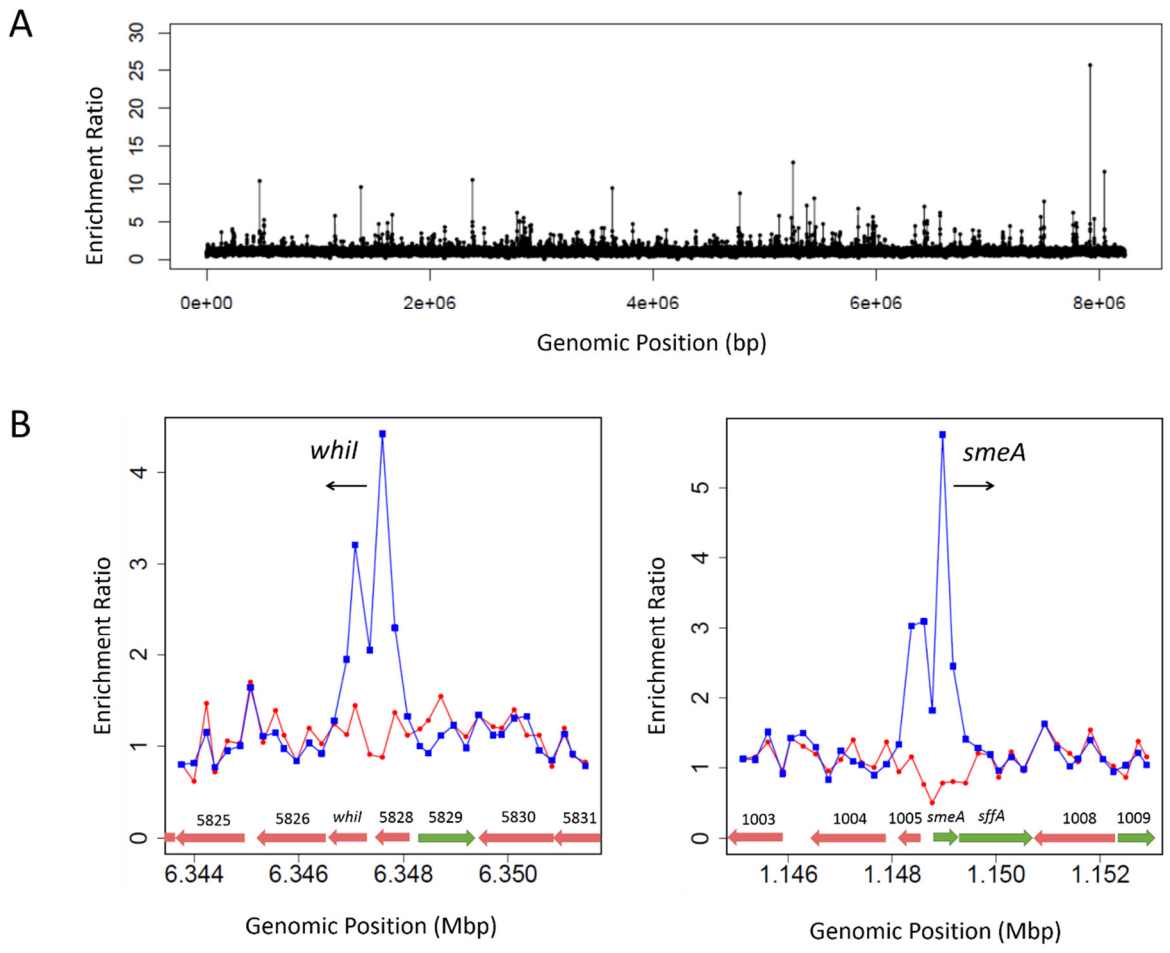
A
Enrichment Ratio
0
5
10
15
20
25
30
0e+00
2e+06
4e+06
6e+06
8e+06
Genomic Position (bp)
B
whiI
Enrichment Ratio
0
1
2
3
4
5825
5826
whiI
5828
5829
5830
5831
6.344
6.346
6.348
6.350
Genomic Position (Mbp)
smeA
Enrichment Ratio
0
1
2
3
4
5
1003
1004
1005
smeA
sffA
1008
1009
1.146
1.148
1.150
1.152
Genomic Position (Mbp)

FIG 5.

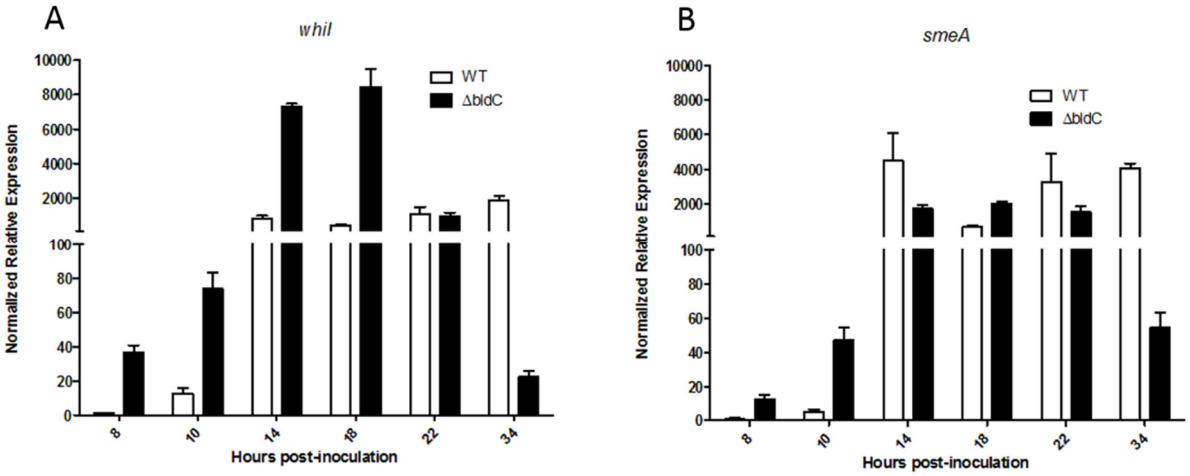
A
whiI
WT
ΔbldC
Normalized Relative Expression
10000
8000
6000
4000
2000
100
80
60
40
20
0
8
10
14
18
22
34
Hours post-inoculation
B
smeA
WT
ΔbldC
Normalized Relative Expression
10000
8000
6000
4000
2000
100
80
60
40
20
0
8
10
14
18
22
34
Hours post-inoculation

FIG 6.

367 **Supplemental Material**

368 **Table S1.** ChIP-chip data set for *S.venezuelae* BldC. Each row represents an enriched probe
369 (probeID) with the mid-position (midpos) of each probe on the *S. coilicolor* genome recorded.
370 Enrichment ratios are expressed as the log-fold change (logFC). Probes are listed in order of
371 significance (adjusted p value - adj.P.Val). For each probe, the nearest gene to the left and right
372 is identified (left/rightLocusTag), its distance to the midpos of the probe (left/rightDistance),
373 whether the gene is on the forward (1) or reverse (-1) strand (inStrand) and the predicted
374 function (left/rightProduct) based on annotation in strepdb
375 (http://strepdb.streptomyces.org.uk). If the midpos of a probe falls within a gene, it's gene
376 identifier (inLocusTag), distance to the probe (inDistance), whether the gene is on the forward
377 (1) or reverse (-1) strand (inStrand) and predicted function (inProduct) is also listed.

378

379 **Table S2.** Strains, Plasmids and Oligonucleotide primers used in this study

380

381 **Movie S1.** Time-lapse microscopy of the wild type strain carrying the FtsZ-YPet fusion. DIC
382 (A) and YFP-channel (B) movies are at 5 frames per second. The time following the first image
383 is indicated at the bottom left. Images were taken every 30 minutes (DIC 150 ms; YFP 100
384 ms). Movies were assembled in the Fiji software package (http://fiji.sc/Fiji).

385

386 **Movie S2.** Time-lapse microscopy of the *bldC* mutant carrying the FtsZ-YPet fusion. DIC (A)
387 and YFP-channel (B) movies are at 5 frames per second. The time following the first image is
388 indicated at the bottom left. Images were taken every 30 minutes (DIC 150 ms; YFP 100 ms).
389 Movies were assembled in the Fiji software package (http://fiji.sc/Fiji).

390

391 **Movie S3.** Time-lapse microscopy of the complemented strain carrying the FtsZ-YPet fusion.
392 DIC (A) and YFP-channel (B) movies are at 5 frames per second. The time following the first
393 image is indicated at the bottom left. Images were taken every 30 minutes (DIC 150 ms; YFP
394 100 ms). Movies were assembled in the Fiji software package (http://fiji.sc/Fiji).
395